HHS Public Access

Author manuscript

Environ Pollut. Author manuscript; available in PMC 2021 December 01.

Published in final edited form as:

Environ Pollut. 2020 December ; 267: 115597. doi:10.1016/j.envpol.2020.115597.

The role of miR-21 in nickel nanoparticle-induced MMP-2 and MMP-9 production in mouse primary monocytes: *in vitro* and *in vivo* studies

Yiqun Mo[a,*], **Yue Zhang**[a,*], **Luke Mo**[a], **Rong Wan**[a], **Mizu Jiang**[a], **Qunwei Zhang**[a]

[a]Department of Environmental and Occupational Health Sciences, School of Public Health and Information Sciences, University of Louisville, Louisville, KY, USA

Abstract

Exposure to metal nanoparticles causes both pulmonary and systemic effects. Nanoparticles can enter the circulation and act directly or indirectly on blood cells, such as monocytes. Monocytes/macrophages are among the first cells to home to inflammatory sites and play a key role in the immune response. Here we investigated the effects of nickel nanoparticles (Nano-Ni), partially [O]-passivated Nano-Ni (Nano-Ni-P), and carbon-coated Nano-Ni (Nano-Ni-C) on MMP-2 and MMP-9 production in mouse primary monocytes both *in vitro* and *in vivo* and explored the potential mechanisms involved. The dose- and time-response studies showed that exposure of primary monocytes from wild-type (WT) mice to 30 μg/mL of Nano-Ni for 24 h caused significant MMP-2 and MMP-9 production; therefore, these dose and time point were chosen for the

Address Correspondence to: Qunwei Zhang, MD, MPH, PhD, Department of Environmental and Occupational Health Sciences, School of Public Health and Information Sciences, University of Louisville, 485 E. Gray Street, Louisville, KY 40202, Tel: (502)852-7200 Fax: (502)852-7246, Qunwei.Zhang@louisville.edu.

Authors' contribution

YM, YZ, and LM prepared and performed the experiments, and contributed to acquisition of data. YM, YZ, RW and MJ analyzed the data and interpreted the results. QZ conceived and supervised the study. The manuscript was written by YM and YZ, and revised critically by QZ. All authors read and approved the final manuscript.

*Mo, Y. and Zhang, Y. contributed equally to this work.

Conflict of interest

The authors declare that they have no conflict of interest.

Ethics approval

The protocols and the use of animals were approved by and in accordance with the University of Louisville Animal Care and Use Committee.

Consent to participate

Not applicable.

Consent for publication

Not applicable.

Availability of data and material

All data and materials are included in the manuscript.

Code availability

Not applicable.

Declaration of interests

The authors declare that they have no known competing financial interests or personal relationships that could have appeared to influence the work reported in this paper.

The authors declare the following financial interests/personal relationships which may be considered as potential competing interests:

following *in vitro* studies. Nano-Ni and Nano-Ni-P caused miR-21 upregulation, as well as MMP-2, MMP-9, TIMP-1 and TIMP-2 upregulation in monocytes from WT, but not miR-21 knock-out (KO), mice, indicating the important role of miR-21 in Nano-Ni-induced MMPs and TIMPs upregulation. However, Nano-Ni-C did not cause these effects, suggesting surface modification of Nano-Ni, such as carbon coating, alleviates Nano-Ni-induced miR-21 and MMPs upregulation. These results were further confirmed by *in vivo* studies by intratracheal instillation of nickel nanoparticles into WT and miR-21 KO mice. Finally, our results demonstrated that exposure of primary monocytes from WT mice to Nano-Ni and Nano-Ni-P caused downregulation of RECK, a direct miR-21 target, suggesting the involvement of miR-21/RECK pathway in Nano-Ni-induced MMP-2 and MMP-9 production.

Graphical Abstract

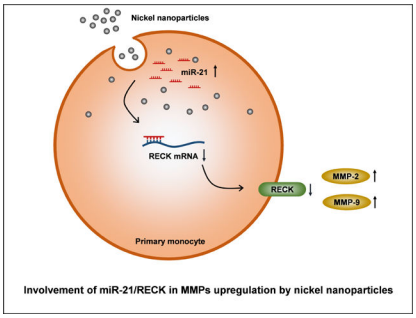

Keywords

Nickel nanoparticles (Nano-Ni); miR-21; monocytes; MMP-2; MMP-9

1. Introduction

With the advancement of nanotechnology, a variety of transition metal nanoparticles are being developed and produced. Nanoparticles are widely used in industry and in medical and medicinal applications. As an important member of the transition metal nanoparticles, nano-sized nickel has found wide-ranging applications in batteries, electrical conductors, permanent magnets, magnetic fluids, magnetic recording media, solar energy absorption, fuel cells, and catalysts (Bajpai et al., 2012; Imran Din and Rani, 2016; Lei et al., 2016; Lu et al., 2007; Wang et al., 2007). Due to their unique chemical and physical properties, nickel alloy nanomaterials have received special interest in biomedical applications, such as biosensor, MRI, and magnetic hyperthermia (Kale et al., 2012; Rana et al., 2005). As the use of nanomaterials continues to expand, the risk of environmental and occupational contamination by nanoparticles is increasing. Therefore, the potential health effects of nickel nanoparticles cannot be ignored. For example, nickel nanoparticles have caused sensitization in a worker without special respiratory protection or control measures (Journeay and Goldman, 2014) and even caused the death of a man who was spraying nickel nanoparticles onto bushes for turbine bearings using a metal arc process by acute respiratory distress syndrome (ARDS) and systemic effects (Phillips et al., 2010).

Previous studies have shown that nanoparticles can penetrate rapidly through the epithelium into the endothelium (Nemmar et al., 2002; Nemmar et al., 2003; Nemmar et al., 2001). They may enter the circulatory system and cause health effects in extra-pulmonary organs (Nemmar et al., 2002; Nemmar et al., 2003; Nemmar et al., 2001; Oberdorster et al., 2005). Notable, individuals exposed to Nano-Ni by inhalation do not only manifest pulmonary effects, but also exhibit systemic effects (Phillips et al., 2010). This raises the intriguing possibility that metal nanoparticles could enter circulation and produce direct or indirect effects on blood cells, such as monocytes, that are more abundant in the systemic circulation. Monocytes are produced by the bone marrow from hematopoietic stem cell precursors called monoblasts (Auffray et al., 2009). They are released into the circulation and mature into different types of macrophages and myeloid lineage dendritic cells at different anatomical locations (Auffray et al., 2009). Monocytes/macrophages are among the first cells to home to inflammatory sites, and they play a key role in the immune response. However, few published reports investigated the molecular mechanisms underlying the effects of metal nanoparticles on leukocytes, especially monocytes.

Matrix metalloproteinases (MMPs) belong to a large family of zinc-dependent natural endopeptidases, which are essential for proper extracellular matrix (ECM) remodeling (Nagase et al., 2006). Mounting evidence suggest that MMPs play a key role in normal and pathological processes, including embryogenesis, wound healing, inflammation, arthritis, cardiovascular disease, and cancer (Birkedal-Hansen, 1995; Greenlee et al., 2007; Nagase et al., 2006; Parks, 2003; Parks and Shapiro, 2001). Among the MMPs, the 72 kDa gelatinase A (MMP-2) and the 92 kDa gelatinase B (MMP-9) are believed to be critical enzymes for degrading type IV collagen, a major component of basement membrane (Birkedal-Hansen, 1995; Nagase et al., 2006). Our previous studies showed that exposure of human monocyte U937 to metal nanoparticles, such as nickel nanoparticles (Nano-Ni) and cobalt nanoparticles (Nano-Co), resulted in increased MMP-2 and MMP-9 expression and activity (Wan et al., 2011; Wan et al., 2008). Intratracheal instillation of Nano-Ni into mouse lungs caused increased MMP-2 and MMP-9 production in lung tissues and increased secretion in BALF (Mo et al., 2019a). In this study, we investigated the mechanisms underlying the alteration of MMPs expression and activity in monocytes induced by Nano-Ni. We also investigated whether surface modification of nickel nanoparticles may have fewer or controllable effects on MMPs expression and activity. Surface modifications may preserve some unique properties of Nano-Ni while reducing its potential health effects. Understanding how Nano-Ni induces changes in the MMP/TIMP system that result in matrix breakdown may lead to interventions that delay or prevent the health effects of Nano-Ni, and examining how surface modification in turn influences these responses allows us to interrogate potential mechanisms.

MicroRNAs (miRNAs) are non-coding, single-stranded RNAs of ~22 nucleotides and constitute a novel class of gene regulators. miRNAs modulate gene expression either directly through translational repression, or by mRNA degradation, utilizing partial or perfect complementarity to the 3′-untranslated region of their targets (Ambros, 2004; Bartel, 2004). In humans, it is estimated that 20–30% of all genes are targeted by miRNAs (Krek et al., 2005; Lewis et al., 2005). To date, several hundred miRNAs have been identified, and each is thought to have hundreds of targets, accounting for the great complexity of their functions

(Nourse et al., 2018). microRNA-21 (miR-21) is one of the miRNAs that have been widely explored. Previous studies have suggested an important role of miR-21 in the regulation of MMP-2 and MMP-9 (Cardozo et al., 2018; Fan et al., 2014; Giovannetti et al., 2010; Li and Li, 2013; Moriyama et al., 2009; Reis et al., 2012).

Reversion-inducing cysteine-rich protein with Kazal motifs (RECK) is a protease inhibitor-like molecule that has been found to be anchored to the cell membrane. The human RECK gene is mapped to chromosome 9p12–13, and its mRNA expression has been found in a wide variety of normal human tissues and untransformed cells, but undetectable in malignant cell lines and oncogenically transformed cells (Takahashi et al., 1998). It is reported that RECK is a direct target of miR-21 (Gabriely et al., 2008). RECK is also demonstrated to negatively regulate MMP-2 and MMP-9 in two ways: suppression of MMP-2/9 secretion from the cells and direct inhibition of its enzymatic activity (Oh et al., 2001; Takahashi et al., 1998).

In the present study, we investigated whether Nano-Ni activated primary monocytes obtained from mouse peripheral blood, altering the expression and activity of MMP-2 and MMP-9 through upregulation of miR-21, which directly targets RECK. We also examined whether surface modification of Nano-Ni such as carbon-coating could ameliorate Nano-Ni-induced activation of MMP-2 and MMP-9 and its possible underlying mechanisms.

2. Materials and methods

2.1. Nickel nanoparticles and their characterizations

Nano-Ni was obtained from Inabata & Co., Ltd., Vacuum Metallurgical Co., Ltd., Japan, while Nano-Ni-P and Nano-Ni-C were purchased from US Research Nanomaterials, Inc., Houston, TX, USA. All three kinds of nickel nanoparticles have a mean diameter of 20 nm. Nano-Ni is composed of 85–90% of metal nickel (Ni) and 10–15% of nickel oxide (NiO). Nano-Ni-P is partially passivated with [O] (0.85 wt%), while Nano-Ni-C is coated with a carbon layer of 0.47 nm in thickness (C=3.61 wt%, O<0.3%). Their microstructure, composition, average hydrodynamic sizes, Zeta potentials, solubility, and other characteristics of Nano-Ni, Nano-Ni-P, and Nano-Ni-C were described in our previous studies (Mo et al., 2019a; Wan et al., 2011). Briefly, the diameter by transmission electron microscopy (TEM) is 10–30 nm for Nano-Ni, Nano-Ni-P, and Nano-Ni-C, and the specific surface area is 43.8 m^2/g for Nano-Ni and 40.0–60.0 m^2/g for both Nano-Ni-P and Nano-Ni-C. The size of particles and agglomerates in physiological saline was 250 nm for Nano-Ni, 246.4 nm for Nano-Ni-P, and 274.8 nm for Nano-Ni-C determined by dynamic light scattering (DLS). The zeta potential is about 2.0 mV for Nano-Ni, 2.3 mV for Nano-Ni-P, and 2.2 mV for Nano-Ni-C. The solubility is about 24 ppm for Nano-Ni, 5.7 ppm for Nano-Ni-P, and 13 ppm for Nano-Ni-C. Nano-Ni, Nano-Ni-P, and Nano-Ni-C were dispersed in physiological saline, ultrasonicated for 10 min, and vibrated thoroughly prior to each experiment.

2.2. Animals

Eight-week-old male C57BL/6J mice, weighing about 22–28 g, were obtained from the Jackson Laboratory (Bar Harbor, ME, USA). The mice were acclimated for 1–2 weeks before starting the experimental protocol. The miR-21 knock-out (KO) mice (B6;129S6-*Mir21a*^{tm1YoLi}/J) were originally obtained from Dr. Yong Li at University of Louisville and are also commercially available at the Jackson Laboratory currently. The mouse miR-21 allele is located at the 3′UTR of a protein-coding gene TMEM49. In this miR-21 KO mice, a 93 bp sequence of precursor to miR-21 (pre-miR-21) was replaced with a pGK-gb2 *loxPIFRT*-flanked neomycin-resistance cassette (Ma et al., 2011b). The mice were bred in the animal facility of University of Louisville. Mice were housed in an air-conditioned room (temperature of 20 ± 2°C, relative humidity of 60 ± 10%) with a 12 h light and 12 h dark cycle environment and with free access to food and water. Mice were monitored daily for general health. Animal use was reviewed and approved by the University of Louisville Institutional Animal Care and Use Committee.

2.3. Isolation of monocytes from mouse peripheral blood

Isolation of monocytes from mouse peripheral blood used a two-step method. (1) Peripheral blood mononuclear cells (PBMCs) were first isolated by density gradient centrifugation using Ficoll-Paque PLUS solution (GE Healthcare, Piscataway, NJ, USA, density 1.077 g/mL at 20°C, cat. no. 17-1440-02), and (2) monocytes were isolated from PBMCs by magnetic cell sorting method using CD11b MicroBeads (Miltenyi Biotec, Auburn, CA, USA). Briefly, peripheral blood (0.8–1.2 mL per mouse) was drawn via cardiac puncture from anesthetized mice by using a 1 mL syringe with a 28G1/2 needle and transferred to an 1.5 mL tube containing 20 μL of anticoagulant (200 mM EDTA, pH 8.0). The blood was diluted with Buffer I (1xPBS without Ca^{2+} and Mg^{2+}, pH 7.4, and 2 mM EDTA) to 4 mL, overlaid on 3 mL room-temperature Ficoll-Paque PLUS solution, and centrifuged for 40 min at 400 g at room temperature. The PBMC interface was collected using a sterile Pasteur pipette and washed three times with 10 mL Buffer I each time. Cells were re-suspended in 90 μL of Buffer II (1xPBS without Ca^{2+} and Mg^{2+}, pH 7.4, 2 mM EDTA, and 0.5% BSA), and 10 μL of CD11b MicroBeads were added. After incubating on ice for 20 min, the cells were washed with 2 mL of Buffer II, and re-suspended in 500 μL of Buffer II. The cells were then run through an MS column placed in the magnetic field of a MiniMACS Separator (Miltenyi Biotec, Auburn, CA, USA). After washing with 500 μL of Buffer II three times, the column was removed from the Separator and placed on a collection tube. 1 mL Buffer II was pipetted onto the column and the magnetically labeled cells (monocytes) were immediately flushed out by applying the plunger supplied with the column. Typically, 1 mL of blood yielded 50,000–150,000 monocytes. To determine purity and to observe morphologic characterizations of monocytes, cells were spun onto slides by using a Cytocentrifuge (Cytospin® 4, Thermo Scientific, Rockford, IL, USA) and the May-Grünwald Giemsa staining and dual immunofluorescent staining were performed. Using these methods, the isolated monocyte purity based on morphologic criteria by May-Grünwald and Giemsa stains exceeded 80%.

2.4. May-Grünwald Giemsa staining

To observe the morphologic characterizations of monocytes, cytospin slides were stained with May-Grünwald and Giemsa stains. Briefly, the cells were fixed in 100% methanol for 5 min at room temperature, and stained with 0.25% (w/v) May-Grünwald stain (Sigma-Aldrich, St. Louis, MO, USA) for 5 min. After a brief rinse in 1 x PBS, the slides were placed in 1:20 diluted Giemsa Stain Solution (LabChem, Pittsburgh, PA, USA) for 15 min. After rinsing slides briefly in ddH_2O, slides were air dried completely, briefly rinsed in 100% ethanol once, placed in xylene twice (5 min each), mounted, and examined under a light microscope.

2.5. Dual immunofluorescent staining

Monocytes on the cytospin slides were fixed in 10% neutral buffered formalin for 20 min at room temperature. After washing with 1xPBS for three times (5 min each), the nonspecific protein binding was blocked by incubating the cells with 3% BSA, 5% normal donkey serum, and 0.3% Triton X-100 for 30 min at room temperature. Then cells were incubated with primary antibodies CD11b (1:50, cat. no. PA1943, Boster Biological, Pleasanton, CA, USA) with Ly-6G (1:50, cat. no. 551459, BD, San Jose, CA, USA) or Alexa Fluor 488-conjugated F4/80 (1:20, cat. no. MF48020, Invitrogen, Carlsbad, CA, USA). CD11b is a marker of monocytes, while Ly-6G is a marker of neutrophils (Geissmann et al., 2003; Swirski et al., 2006). Activated macrophages exhibited F4/80 positive, while monocytes showed F4/80 low (Geissmann et al., 2003; Swirski et al., 2006). After incubation with primary antibodies for 2 h at room temperature and washed with 1xPBS three times, the cells were incubated with Alexa Fluor 594-conjugated donkey anti-rabbit IgG (1:500, Abcam, Cambridge, MA, USA) with/without Alexa Fluor 488-conjugated donkey anti-rat IgG (1:500, Invitrogen, Carlsbad, CA, USA) at room temperature for 1 h. After washing, the slides were mounted with Prolong Gold Antifade Reagent with DAPI (Invitrogen, Carlsbad, CA, USA) and examined by fluorescence microscopy.

2.6. Exposure of monocytes to nickel nanoparticles

Monocytes isolated from mouse peripheral blood were cultured in RPMI 1640 medium supplemented with 100 U/mL penicillin and 100 μg/mL streptomycin (Mediatech, Manassas, VA, USA). The cells were cultured at 37 °C incubator in the presence of 5% CO_2. After culturing for 4 h, cells were treated with Nano-Ni, Nano-Ni-P, or Nano-Ni-C for various times. Cells without nickel nanoparticle treatment served as controls. After treatment, cells were collected for total RNA or protein isolation, while the culture media were collected for detection of MMP-2 and MMP-9 protein levels by ELISA and their activity by gelatin zymography assay.

2.7. Exposure of mice to nickel nanoparticles

Intratracheal instillation method was used to expose mice to Nano-Ni, Nano-Ni-P, or Nano-Ni-C as described previously (Mo et al., 2019a; Wan et al., 2017; Zhang et al., 1998a; Zhang et al., 1998b; Zhang et al., 2003). Compared to an inhalation study, intratracheal instillation is an easy and reliable method and has been widely used to identify particle toxicity and to compare responses to different particle types (Driscoll et al., 2000). Briefly, mice were

randomly assigned to control or various nickel nanoparticle groups. Under anesthesia, 50 μg per mouse of Nano-Ni or either Nano-Ni-P or Nano-Ni-C with same molar concentration of Ni as Nano-Ni was instilled intratracheally by a syringe with a 28G1/2 needle. Control mice were instilled with physiological saline alone. The mice were sacrificed at day 3 after exposure for isolation of monocytes from peripheral blood.

2.8. Detection of MMP-2 or MMP-9 protein level and activity

The MMP-2 or MMP-9 protein level in the cell culture medium was determined by Mouse MMP-2 or MMP-9 PicoKine™ ELISA Kit (Boster Biological, Pleasanton, CA, USA) according to the manufacturer's instructions, and was interpolated using the standard curve performed on the same plate.

The MMP-2 or MMP-9 activity in the cell culture medium was determined by a gelatin zymography assay as described previously (Mo et al., 2019a; Mo et al., 2009b; Wan et al., 2011; Wan et al., 2008; Zhang et al., 2016; Zhang et al., 2019). A total of 60 μL of culture medium mixture (48 μL medium + 12 μL 5xloading buffer) was loaded in each lane of 10% SDS-PAGE copolymerized with 0.5 mg/mL gelatin, which was used as the substrate under non-reducing conditions. After electrophoresis, the gel was first washed at room temperature in a buffer containing 50 mM Tris-HCl (pH 7.5) and 2.5% Triton X-100 (Sigma, St. Louis, MO, USA) for 1 h with solution changes every 15 min. Then, the gel was incubated at 37 °C overnight in another buffer containing 50 mM Tris-HCl (pH 7.5), 0.2 M NaCl, 7.55 mM $CaCl_2$, 1 μM $ZnCl_2$, and 1% Triton X-100, with gentle shaking, to develop the enzyme activity bands. After washing with distilled water twice, the gel was stained with 0.1% Coomassie Brilliant Blue R-250 (Bio-Rad, Hercules, CA, USA) and destained with 10% acetic acid until the clear bands were observed against the background of Coomassie blue-stained gel.

2.9. Total RNA isolation and real-time PCR

The expression levels of miR-21, MMP-2, MMP-9, TIMP-1, TIMP-2, and RECK in the monocytes after nickel nanoparticle treatment were determined by real-time PCR as described previously (Mo et al., 2009a; Mo et al., 2012). Total RNA was isolated from monocytes by using mirVana miRNA Isolation Kit (Abcam, Cambridge, MA, USA) according to the manufacturer's instruction. And the total RNA concentration was determined by absorbance at 260 nm with a DU 730 Spectrophotometer (Beckman Coulter, Fullerton, CA, USA).

The expression level of miR-21 was determined by using TaqMan® MicroRNA Assay (Assay ID 000397, Applied Biosystems, Foster City, CA, USA). There were two-steps: (1) Reverse transcription by using TaqMan® MicroRNA Reverse Transcription Kit (Applied Biosystems) and (2) Real-time PCR by using TaqMan® Universal PCR Master Mix II (No UNG) (Applied Biosystems). Values of miR-21 expression in monocytes were normalized to the endogenous control U6 snRNA (Assay ID 001973, Applied Biosystems), and reported as fold increase compared to the control without nickel nanoparticle treatment.

The mRNA expression levels of MMP-2, MMP-9, TIMP-1, TIMP-2, and RECK in monocytes after nickel nanoparticle treatment were determined by RT-qPCR by using M-

MLV reverse transcriptase (Promega, Madison, WI, USA) and iTaq Universal SYBR Green Supermix (Bio-Rad, Hercules, CA, USA) as described previously (Mo et al., 2009a; Mo et al., 2012; Mo et al., 2020). Real-time PCR was performed using a Bio-Rad iQ5 iCycler. The experimental protocol consisted of four programs: (i) Denaturation of the cDNA/RNA hybrid at 95 °C for 3 min; (ii) Amplification of cDNA for 40 or 50 cycles, each cycle using sequentially 95 °C for 10 s, 58 °C for 30 or 45 s, and 72 °C for 30 or 45 s; (iii) Analysis of the melting curve to confirm the single product amplification during the PCR assay; and (iv) Cooling the rotor and thermal chamber at 25 °C. The specific primers for each gene were listed in Table 1. The relative expression level of each gene was calculated by using $2^{-\Delta\Delta CT}$ (Livak) method (Livak and Schmittgen, 2001) and normalized to the expression of a reference gene β-actin or GAPDH in the same sample, and expressed as the fold increase of the gene in the nickel nanoparticle-exposed group relative to the control without nickel nanoparticle exposure.

2.10. Protein isolation and Western blot

Protein was isolated from monocytes by using RIPA lysis buffer supplemented with PMSF, protease inhibitor cocktail, and sodium orthovanadate (Santa Cruz Biotechnology, Santa Cruz, CA, USA) according to the manufacturer's instruction. The protein concentration was determined by using Bio-Rad Protein Assay (Bradford method) with a DU730 Spectrophotometer (Beckman Coulter, Fullerton, CA, USA). Western blot was performed as previously described (Feng et al., 2015; Long et al., 2019; Mo et al., 2009a; Mo et al., 2012; Mo et al., 2020; Yu et al., 2010; Zhang et al., 2016). The primary antibody for RECK (1:1000, cat. no. 3433) was obtained from Cell Signaling Technology (Beverly, MA, USA), and for β-actin (1:2000, cat. no. A1978) from Sigma (Saint Louis, MO, USA). HRP-conjugated goat anti-rabbit IgG (1:2000, for RECK) or horse anti-mouse IgG (1:2000, for β-actin) were from Cell Signaling Technology (Beverly, MA, USA). Immunoreactive bands were detected using SuperSignal™ West Pico PLUS Chemiluminescent Substrate (Thermo Scientific, Rockford, IL, USA) followed by exposure to CL-XPosure™ film (Thermo Scientific, Rockford, IL, USA).

2.11. Statistical analysis

Statistical analyses were carried out using SigmaPlot 13.0 software (Systat Software, Inc., San Jose, CA, USA). Data were expressed as the mean ± SEM. Differences among groups were evaluated by one-way or two-way analysis of variance (ANOVA). If necessary, transformation of data was used to achieve normally distributed data before ANOVA analysis. If a p value was less than 0.05, a difference was considered statistically significant.

3. Results

3.1. Characteristics of isolated monocytes

Monocytes are identified as cells ranging between 10 and 30 μm in diameter, with a horseshoe- or kidney-shaped nucleus, a variable nucleus-to-cytoplasm ratio, and fine granules and vacuoles in the cytoplasm (Swirski et al., 2006). In this study, monocytes were isolated from mouse peripheral blood. To observe their morphology and characteristics, the cells were cytospinned onto slides and stained with May-Grünwald and Giemsa stains or by

dual immunofluorescent staining. The isolated monocytes exhibited typical monocyte characteristics (Fig. 1A) and a strong positive when cells were stained with anti-CD11b antibody (Fig. 1B&F), which is in consistent with previous studies (Auffray et al., 2009; Swirski et al., 2006). The isolated cells exhibited low expression of a macrophage marker, F4/80 (Fig. 1G), and were negative when cells were stained with a granulocyte marker Ly-6G (Fig. 1C).

3.2. Effects of Nano-Ni on MMP-2 and MMP-9 protein levels and activities

In order to find an appropriate dose and a time point for the comparative studies of three kinds of nickel nanoparticles, Nano-Ni was chosen to perform the dose-response and time-response studies. Primary monocytes were isolated from the peripheral blood of C57BL/6J mouse, and the effects of Nano-Ni on MMP-2 and MMP-9 protein levels in the conditioned medium were determined by ELISA assay, while their activities were analyzed by gelatin zymography assay. The results of dose-response study showed that when cells were treated with 15 μg/mL of Nano-Ni for 24 h, no significant increase in the MMP-2 and MMP-9 protein levels in the conditioned medium was observed (Fig. 2A–B). However, when cells were treated with 30 μg/mL of Nano-Ni for 24 h, significant increases in the protein levels of MMP-2 and MMP-9 in the conditioned medium was observed as compared to those in the controls (Fig. 2A–B). The results of gelatin zymography assay were consistent with the ELISA results; there was a significant increase in MMP-2 or MMP-9 activity in the conditioned medium of monocytes exposed to 30 μg/mL of Nano-Ni (Fig. 2C). Therefore, a dose of 30 μg/mL of Nano-Ni was selected for the following studies.

In the time-response study, monocytes were treated with 30 μg/mL of Nano-Ni for 12, 24, and 48 h. Although Nano-Ni treatment for 12 h did not cause a significant increase in the MMP-2 and MMP-9 protein levels in the conditioned medium of cultured primary monocytes, their levels were significantly increased when cells were treated with 30 μg/mL of Nano-Ni for 24 and 48 h (Fig. 3A–B). The gelatin zymography assay results also showed significant increases in the activities of MMP-2 and MMP-9 when cells were treated with 30 μg/mL of Nano-Ni for 24 and 48 h (Fig. 3C). Thus, a time point of 24 h was chosen for the following studies.

3.3. Nano-Ni and Nano-Ni-P exposure caused miR-21 upregulation, but Nano-Ni-C did not

Our previous studies showed that Nano-Ni and Nano-Ni-P exposure caused severe pulmonary injury and fibrosis (Mo et al., 2019a). Surface modification of Nano-Ni such as carbon coating (Nano-Ni-C) alleviated Nano-Ni-induced pulmonary injury and fibrosis (Mo et al., 2019a). In order to investigate whether these three kinds of nickel nanoparticles would cause alteration of miR-21 expression in primary monocytes, monocytes isolated from mouse peripheral blood were exposed to Nano-Ni, Nano-Ni-P, or Nano-Ni-C for 24 h, and miR-21 expression was determined by real-time PCR using TaqMan microRNA Assays. The results showed that both Nano-Ni and Nano-Ni-P caused a significant increase in miR-21 expression as compared to that in the control (Fig. 4A). However, Nano-Ni-C did not cause significant miR-21 upregulation (Fig. 4A).

To confirm the results *in vivo*, mice were intratracheally instilled with Nano-Ni, Nano-Ni-P, or Nano-Ni-C. At day 3 after exposure, mice were sacrificed, and monocytes were isolated from peripheral blood. The expression level of miR-21 was assayed by rea-time PCR and the results showed that Nano-Ni and Nano-Ni-P, but not Nano-Ni-C induced miR-21 upregulation (Fig. 4B), which was consistent with the results of the *in vitro* study (Fig. 4A).

3.4. Knocking out miR-21 ameliorated MMP-2 and MMP-9 upregulation induced by Nano-Ni and Nano-Ni-P

To compare the effects of the three kinds of nickel nanoparticles on MMP-2 and MMP-9 expression in the primary monocytes, both *in vitro* and in *vivo* experiments were performed. To explore the role of miR-21 in these effects, miR-21 KO mice were introduced. MMP-2 and MMP-9 were determined at mRNA, protein, and activity levels by using real-time PCR, ELISA, and gelatin zymography assay respectively.

3.4.1. mRNA levels in vitro—Monocytes isolated from wild-type (WT, C57BL/6J) or miR-21 KO mice were treated with three kinds of nickel nanoparticles. The mRNA expression levels of MMP-2, MMP-9, TIMP-1, and TIMP-2 in monocytes were determined by real-time PCR. The results showed that Nano-Ni caused significant increases in the mRNA levels of MMP-2, MMP-9, TIMP-1, and TIMP-2 in monocytes from WT mice. Nano-Ni-P had similar effects as Nano-Ni. However, Nano-Ni-C did not induce significant increases in mRNA levels, which were significantly lower than those in the Nano-Ni group (Fig. 5). In monocytes obtained from miR-21 KO mice, all three kinds of nickel nanoparticles, including Nano-Ni, Nano-Ni-P, and Nano-Ni-C, did not cause significant increases in MMP-2, MMP-9, TIMP-1, and TIMP-2 mRNA expression (Fig. 5).

3.4.2. Protein and activity levels in vitro—The MMP-2 and MMP-9 protein levels in the conditioned medium of cultured monocytes were determined by ELISA, while their activities were determined by gelatin zymography assay. The results showed that in the conditioned medium from WT monocytes, both Nano-Ni and Nano-Ni-P caused significant increases in both MMP-2 and MMP-9 protein levels as compared to those in the controls (Fig. 6A–B). Although Nano-Ni-C also caused a significant increase in MMP-9, but not MMP-2, protein level, their levels were significantly lower than those in the Nano-Ni group (Fig. 6A–B). However, in the conditioned medium from cultured miR-21 KO monocytes, although Nano-Ni or Nano-Ni-P caused significant increases in MMP-2 or MMP-9 protein levels, their levels were significantly lower than those in the conditioned medium from WT monocytes with the same treatment (Fig. 6A–B). Nano-Ni-C did not cause a significant increase in MMP-2 and MMP-9 protein levels in the conditioned medium from cultured miR-21 KO monocytes (Fig. 6A–B). The results of MMP-2 and MMP-9 activities were consistent with their protein results (Fig. 6C).

3.4.3. mRNA levels in vivo—For the *in vivo* experiments, WT or miR-21 KO mice were intratracheally instilled with 50 μg/mL of Nano-Ni, or with either Nano-Ni–P or Nano-Ni–C with same molar concentration of Ni as Nano-Ni. At day 3 after exposure, mice were sacrificed, and monocytes were isolated from the mouse peripheral blood. The mRNA expression of MMP-2, MMP-9, TIMP-1, and TIMP-2 were determined by real-time PCR.

The results showed that the expression of MMP-2, TIMP-1, and TIMP-2 were significantly upregulated in monocytes isolated from WT mice with Nano-Ni or Nano-Ni-P exposure, but not with Nano-Ni-C exposure (Fig. 7A, C–D). Nano-Ni and Nano-Ni-P, but not Nano-Ni-C, caused a non-statistically significant increase in MMP-9 mRNA expression in monocytes from WT mice (Fig. 7B). However, in monocytes from miR-21 KO mice exposed to Nano-Ni or Nano-Ni-P, the mRNA expression of MMP-2 and TIMP-2 were significantly lower than those in the WT monocytes with the same treatments (Fig. 7A&D).

3.5. Exposure to Nano-Ni or Nano-Ni-P caused RECK downregulation

The RECK gene is an endogenous matrix metalloproteinase (MMP) inhibitor, and it regulates at least three members of the MMPs family: MMP-2, MMP-9, and MT1-MMP (Oh et al., 2001; Takahashi et al., 1998). It is one of the direct targets of miR-21 (Gabriely et al., 2008). The expression level of RECK was determined by both real-time PCR and Western blot. The results showed that exposure to Nano-Ni or Nano-Ni-P caused significant downregulation of RECK in the monocytes isolated from WT mice in both *in vitro* and *in vivo* settings, but not in monocytes isolated from miR-21 KO mice (Fig. 8). Exposure to Nano-Ni-C did not alter RECK expression (Fig. 8).

4. Discussion

Our study has demonstrated that exposure to Nano-Ni and Nano-Ni-P caused MMP-2, MMP-9, and miR-21 upregulation and RECK downregulation in primary peripheral blood monocytes obtained from WT, but not miR-21 KO, mice, suggesting MMP-2 and MMP-9 upregulation induced by Nano-Ni and Nano-Ni-P may be through miR-21 upregulation and RECK downregulation. These *in vitro* study results were further confirmed by *in vivo* study, in which mice were intratracheally instilled with nickel nanoparticles, indicating an extra-pulmonary effect of Nano-Ni and Nano-Ni-P exposure. Our previous study has demonstrated that intratracheal instillation of Nano-Ni caused severe pulmonary inflammation and fibrosis, and surface modification of Nano-Ni such as carbon coating alleviated Nano-Ni-induced effects (Mo et al., 2019a). In this study, carbon-coating nickel nanoparticles did not cause significant upregulation of MMP-2 and MMP-9, suggesting a protective role of surface modification such as carbon-coating in Nano-Ni-induced injury.

Monocytes are a type of leukocyte in the blood and can differentiate into macrophages and myeloid lineage dendritic cells in the tissues. Phagocytic cells, such as mononuclear phagocytes (monocytes/macrophages) and granulocytes, are the first cells that interact with particles and pathogens in the bloodstream and thereby represent the immune system’s first line of defense. Activated mononuclear phagocytes play a potent role in immune reactions by releasing reactive oxygen species (ROS), reactive nitrogen species (RNS), and cytokines, such as IL-1β, IL-6, IL-10, CXCL8 and TNFα (Auffray et al., 2009; Serbina et al., 2008). Although our and other previous studies showed that exposure of human monocyte-like cell lines, such as U937 and THP-1, to metal nanoparticles caused cytokine production and MMPs activation (Foldbjerg et al., 2009; Murphy et al., 2016; Rueda-Romero et al., 2016; Senapati et al., 2015; Wan et al., 2011; Wan et al., 2008), previous studies focused and limited on *in vitro* studies and cell lines. Few studies investigated the effects of metal

nanoparticles on primary monocytes and performed both *in vitro* and *in vivo* experiments. In this study, we determined the effects of nickel nanoparticles on primary monocytes isolated from mouse peripheral blood. The data obtained from using primary cells is more relevant and reflective of the *in vivo* environment. Therefore, our using both *in vitro* and *in vivo* settings to study the effects of nickel nanoparticles on the monocytes is a highly integrated approach.

Matrix metalloproteinases (MMPs) constitute a multigene family of secreted and cell surface enzymes that regulate a wide range of cellular events, including extracellular matrix (ECM) remodeling, cell surface proteolysis, intracellular signal transduction, regulation of paracrine signals, and generation and inactivation of bioactive molecules (Nagase et al., 2006; Sternlicht and Werb, 2001). Among them, MMP-2 and MMP-9, also known as gelatinases A and B due to their characteristic activities, are enzymes which degrade gelatin as well as a number of ECM molecules including type IV, V and XI collagens, laminin, aggrecan core protein, etc (Nagase et al., 2006; Sternlicht and Werb, 2001). Type IV collagen is a main component of basement membranes, a dense layer of ECM that separate epithelium or endothelium from stroma (Morrissey and Sherwood, 2015). Here, our *in vitro* study revealed that MMP-2 and MMP-9 protein levels and their activities were increased after Nano-Ni or Nano-Ni-P exposure in mouse peripheral blood monocytes, which is consistent with our previous study by using human monocyte-like cell line U937 (Wan et al., 2011). An interesting finding was that MMP-2 and MMP-9 expression levels were upregulated in primary monocytes isolated from mouse peripheral blood at day 3 after intratracheal Nano-Ni or Nano-Ni-P instillation, implicating intratracheal instillation of Nano-Ni or Nano-Ni-P into mouse lungs induced systemic effects. This phenomenon can be explained by the following two points of view. (1) Intratracheal instillation of Nano-Ni causes upregulation of proinflammatory cytokines such as IL-1β, IL-6, and TNFα in mouse lungs (Mo et al., 2020; Zhang et al., 1998a; Zhang et al., 2003), which enter the blood stream and circulate throughout the body, causing peripheral blood monocyte activation and extra-pulmonary tissue and organ inflammation. A variety of physiologic stimuli have been described to initiate or enhance MMP-2 and MMP-9 gene expression in diverse cell types. These factors include inflammatory cytokines such as TGF-β1, IL-1, and TNFα (Overall et al., 1991; Ries et al., 1994; Ries and Petrides, 1995). (2) Nano-Ni or Nano-Ni-P intratracheally instilled into lungs can directly penetrate alveolar membranes and translocate to the circulation and other tissues because of their small size, which may result in adverse effects in extra-pulmonary organs. Our previous study has demonstrated that intratracheal instillation of Nano-Ni or Nano-Co into rat lungs caused peripheral blood neutrophil activation, resulting in secretion of TNFα, MIP-2, and NO (Mo et al., 2008). Intratracheal instillation of Nano-Ni or Nano-Ni-P also caused increased MMP-2 and MMP-9 protein levels and activities in mouse lungs and BALF (Mo et al., 2019a). Induction of MMP-2 and MMP-9 levels in both peripheral blood monocytes and the lungs promotes direct monocytes migration across reconstituted basement membranes, providing a potential mechanism in extravasation of monocytes into injured lungs *in vivo* and alveolar macrophage recruitment and accumulation in the lungs after Nano-Ni exposure.

In this study, we found that Nano-Ni and Nano-Ni-P exposure caused miR-21 upregulation in mouse primary peripheral blood monocytes both *in vitro* and *in vivo*. Several pathways or

mechanisms have been reported to upregulate miR-21, including signal transducer and activator of transcription 3 (STAT3) (Loffler et al., 2007). The miR-21 gene contains two conserved STAT3 binding sites within its enhancer region and is induced by interleukin 6 (IL-6) in a STAT3-dependent way (Loffler et al., 2007). Our and other previous studies have shown that metal nanoparticles intratracheally instilled into lungs caused upregulation of proinflammatory cytokines such as IL-6, IL-1β, and TNFα (Bai et al., 2018; Mo et al., 2020; Sager et al., 2016; Zhang et al., 1998a; Zhang et al., 2003). Hypoxia is another factor that can consistently induce miR-21 upregulation (Krichevsky and Gabriely, 2009; Shen et al., 2013). Hypoxia inducible factor 1α (HIF-1α) is a major mediator of cell response to hypoxia and the HIF-1α-binding site is present in the pri-miR-21 promoter (Krichevsky and Gabriely, 2009). Nickel is known to mimic hypoxia through activation of HIF-1α (Maxwell and Salnikow, 2004; Salnikow et al., 2002; Wan et al., 2011). Our previous studies showed that Nano-Ni exposure resulted in cell hypoxia and HIF-1α accumulation in the nucleus of human monocyte U937 (Wan et al., 2011). In addition, accumulating evidence suggests a close connection between ROS signaling and microRNA (miRNA) pathways. Some miRNAs, so called ROSmirs, are regulated by oxidative stress to mediate expression levels of their direct targets in response to ROS (He and Jiang, 2016). For example, exposure of macrophage cell line RAW 246.7 to exogenous H_2O_2 caused alteration of miRNA expression levels, including upregulation of miR-21 (Thulasingam et al., 2011). ROS are often generated within inflammatory environment to activate NF-κB in cells by various mechanisms (Hoesel and Schmid, 2013). Several miRNAs, including miR-21, have been validated to be directly transcriptionally regulated by NF-κB (Ma et al., 2011a; Niu et al., 2012). Therefore, NF-κB activation might be one of mechanisms for ROS-mediated miR-21 induction. Many environmental agents have been proved to be sources of ROS. ROS-induced miR-21 upregulation is involved in arsenic-induced cell malignant transformation, and NF-κB mediates miR-21 induction upon ROS exposure by binding directly to the promoter region of miR-21 gene (Ling et al., 2012). Our previous studies showed that Nano-Ni exposure caused oxidative stress (Mo et al., 2019b; Zhang et al., 1998a; Zhang et al., 1998b; Zhang et al., 2003). Nano-Ni exposure caused significant increases in thiobarbituric acid reactive substances (TBARS) and genomic DNA 8-OHdG in mouse lung tissues. Nano-Ni–P had similar effects as Nano-Ni. However, Nano-Ni–C only caused a slight, but not significant, increase in the levels of TBARS and 8-OHdG (Mo et al., 2019a). This may in part explain why Nano-Ni and Nano-Ni-P caused miR-21 upregulation, but Nano-Ni-C not in the present study. Taken together, several pathways such as STAT3/IL-6 pathway, HIF-1α pathway, oxidative stress, et al., may all possibly account for miR-21 overexpression in mouse primary peripheral blood monocytes after Nano-Ni and Nano-Ni-P exposure.

Reversion-inducing cysteine-rich protein with Kazal motifs (RECK) is widely expressed in various human organs (Takahashi et al., 1998). It has the ability to regulate at least three members of the MMP family: MMP-2, MMP-9, and MT1-MMP (Oh et al., 2001; Takahashi et al., 1998). RECK expression inversely correlates with MMP-2 and MMP-9 expression levels (Oh et al., 2001; Takahashi et al., 1998). In the absence of RECK expression, excess MMP activity results in excessive degradation of the ECM, causing reduced structural integrity (Oh et al., 2001; Takahashi et al., 1998). In this study, we found that Nano-Ni or Nano-Ni-P induced RECK downregulation in WT, but not in miR-21 KO monocytes, which

allows the MMPs to elicit their full activity. We also found miR-21 upregulation in mouse primary peripheral blood monocytes. RECK is reported to be a direct target of miR-21, which negatively regulates the mRNA and protein levels of RECK (Gabriely et al., 2008). Thus, our study demonstrated that MMP-2 and MMP-9 upregulation induced by Nano-Ni and Nano-Ni-P may be due to RECK downregulation caused by miR-21 upregulation.

In this study, we found that RECK was downregulated, but TIMP-1 and TIMP-2 were upregulated in monocytes after Nano-Ni and Nano-Ni-P exposure. TIMPs are a group of smaller (20–30 kDa) MMP inhibitors and four TIMPs (TIMP-1 to TIMP-4) have been identified and characterized (Brew et al., 2000). Previous studies suggest that RECK shares little functional redundancy with the TIMPs based on the following two reasons: (1) RECK is membrane-anchored, while TIMPs are secreted; and (2) the lack of RECK is embryonic lethal in mice, while the lack of TIMP-1 or TIMP-2 has little effect on development (Caterina et al., 2000; Nothnick et al., 1997; Oh et al., 2001; Takahashi et al., 1998; Wang et al., 2000). Strong expression and synthesis of TIMP-1 and TIMP-2, as well as upregulation of MMP-2 and membrane type 1 MMP (MT1-MMP), have been found in bone marrow–derived human mesenchymal stem cells (hMSCs) (Ries et al., 2007). It is possible that MMP-2 and MMP-9 upregulation induced by Nano-Ni or Nano-Ni-P elicited upregulation of TIMPs, which in turn inhibit MMPs action. On the other hand, MMP-2 proenzyme forms a tight complex with TIMP-2 and its activation on the cell surface requires both TIMP-2 and membrane-type 1 MMP (MT1-MMP) (MMP-14) (Caterina et al., 2000; Itoh et al., 2001; Wang et al., 2000). The hemopexin domain of proMMP-9 also forms a tight complex with TIMP-1 and TIMP-3 through their C-terminal domains (Nagase et al., 2006). Although TIMPs are endogenous inhibitors of MMPs, the balance between MMPs and TIMPs are critical for the eventual ECM remodeling in the tissue.

The physico-chemical properties of metal nanoparticles, such as small size, high surface area, etc., are useful for many applications in medicine, chemistry, material science and physics. However, these physico-chemical characteristics may also be associated with undesired health effects that may be different from the bulk materials. Increasing evidence indicates that as particle size decreases, some metal nanoparticles exhibit increased toxicity, even if the material is relatively inert in its bulk form (e.g., Ag, Au, and Cu) (Galdiero et al., 2011; Schrand et al., 2010). These responses appear to be dependent on the physical and chemical properties of the particles, such as particle size, shape, high surface area to volume ratio, chemical composition, crystallinity, electronic properties, surface functional groups, solubility, aggregation behavior, dissolution behavior, surface reactivity and binding ability (Beddoes et al., 2015; Johnston et al., 2010; Shin et al., 2015). Our previous studies showed that surface modification of Nano-Ni such as carbon coating significantly alleviates Nano-Ni-induced acute and chronic pulmonary inflammation and fibrosis (Mo et al., 2019a). In the present study, we presented a comparative assessment of the effects of Nano-Ni, Nano-Ni-P, and Nano-Ni-C, which have the same diameter and surface area, but differential surface modification, on mouse primary peripheral blood monocytes. The results showed that Nano-Ni and Nano-Ni-P exposure caused miR-21 upregulation, but Nano-Ni-C did not. The results were further confirmed by the *in vivo* study. Both *in vitro* and *in vivo* results also showed that Nano-Ni and Nano-Ni-P, but not Nano-Ni-C, exposure caused MMP-2 and MMP-9 upregulation. These results suggest that different kinds of surface modification will

have different effects; carbon coating (Nano-Ni-C), but not partially passivated (Nano-Ni-P), could reduce Nano-Ni-induced upregulation of MMP-2 and MMP-9, which is through Nano-Ni-induced upregulation of miR-21.

In the present study, the intratracheal instillation method was used for nickel nanoparticle exposure. Although inhalation exposure provides a natural route of entry into the host and, as such, is the preferred method for the introduction of toxicant into the lungs, inhalation exposure cannot always to be used due to various reasons, and the direct instillation of the test materials into lungs via the trachea has been employed in many studies as an alternative exposure procedure (Bai et al., 2018; Driscoll et al., 2000; Mo et al., 2019a; Nemmar et al., 2003; Nemmar et al., 2001; Wan et al., 2017; Zhang et al., 1998a; Zhang et al., 1998b; Zhang et al., 2003). Intratracheal instillation has dominated pulmonary toxicity studies of various particles, due in part to its relative ease and cost efficiency as compared with inhalation exposure protocol. It also offers the important advantage that the toxic effects of particle extracts may easily be investigated (Driscoll et al., 2000).

Taken together, our study herein demonstrated that exposure to Nano-Ni and Nano-Ni-P caused increased mRNA expression and protein activity of MMP-2 and MMP-9 in primary mouse peripheral blood monocytes *in vitro* and *in vivo*. Exposure of primary monocytes to Nano-Ni and Nano-Ni-P also caused miR-21 upregulation, which may further downregulate RECK expression and finally upregulate MMP-2 and MMP-9. In addition, our results also demonstrated that alteration of physiochemical properties of nickel nanoparticles by surface modification, such as carbon coating, may have different effects on monocytes. The Nano-Ni-induced upregulation of miR-21 may be alleviated through surface modification, which may further reduce Nano-Ni-induced activation of MMPs. The results not only provide an understanding of the potential systemic toxic effects of nickel nanoparticle exposure and but also suggest an important role of surface properties in the mechanisms of Nano-Ni-induced toxicity. However, the detailed mechanisms of how Nano-Ni caused upregulation of miR-21 and the phenotypic and functional changes of blood monocytes after nickel nanoparticle exposure still need to be further explored.

Acknowledgements

The results were presented in part at 2017 Society of Toxicology (SOT) Annual Conference; March 12–16, 2017; Baltimore, MD, USA.

Funding

This work was partly supported by NIH (ES023693, ES028911, and HL147856), KSEF-148-RED-502-16-381, and Kentucky Lung Cancer Research Program to Dr. Qunwei Zhang.

Abbreviations:

(Nano-Ni)	Nickel nanoparticles
(Nano-Ni-P)	Partially passivated nickel nanoparticles
(Nano-Ni-C)	Carbon-coated nickel nanoparticles
(WT)	Wild-type

(KO)	Knock-out
(miR-21)	microRNA-21
(MMP-2)	Matrix metalloproteinase-2
(MMP-9)	Matrix metalloproteinase-9
(TIMP-1)	Tissue inhibitor of metalloproteinase-1
(TIMP-2)	Tissue inhibitor of metalloproteinase-2
(ECM)	Extracellular matrix
(RECK)	Reversion-inducing cysteine-rich protein with Kazal motifs
(IL-1β)	Interleukin 1 beta
(IL-6)	Interleukin 6
(IL-10)	Interleukin 10
(TNFα)	Tumor necrosis factor alpha
(TGF-β1)	Transforming growth factor beta 1
(HIF-1α)	Hypoxia inducible factor 1α
(DAPI)	4′,6-diamidino-2-phenylindole
(ROS)	Reactive oxygen species

References

Ambros V, 2004 The functions of animal microRNAs. Nature 431, 350–355. [PubMed: 15372042]

Auffray C, Sieweke MH, Geissmann F, 2009 Blood monocytes: development, heterogeneity, and relationship with dendritic cells. Annu Rev Immunol 27, 669–692. [PubMed: 19132917]

Bai KJ, Chuang KJ, Chen JK, Hua HE, Shen YL, Liao WN, Lee CH, Chen KY, Lee KY, Hsiao TC, Pan CH, Ho KF, Chuang HC, 2018 Investigation into the pulmonary inflammopathology of exposure to nickel oxide nanoparticles in mice. Nanomedicine 14, 2329–2339. [PubMed: 29074311]

Bajpai R, Roy S, kulshrestha N, Rafiee J, Koratkar N, Misra DS, 2012 Graphene supported nickel nanoparticle as a viable replacement for platinum in dye sensitized solar cells. Nanoscale 4, 926–930. [PubMed: 22193832]

Bartel DP, 2004 MicroRNAs: genomics, biogenesis, mechanism, and function. Cell 116, 281–297. [PubMed: 14744438]

Beddoes CM, Case CP, Briscoe WH, 2015 Understanding nanoparticle cellular entry: A physicochemical perspective. Adv Colloid Interface Sci 218, 48–68. [PubMed: 25708746]

Birkedal-Hansen H, 1995 Matrix metalloproteinases. Adv Dent Res 9, 16. [PubMed: 8934944]

Brew K, Dinakarpandian D, Nagase H, 2000 Tissue inhibitors of metalloproteinases: evolution, structure and function. Biochim Biophys Acta 1477, 267–283. [PubMed: 10708863]

Cardozo ER, Foster R, Karmon AE, Lee AE, Gatune LW, Rueda BR, Styer AK, 2018 MicroRNA 21a-5p overexpression impacts mediators of extracellular matrix formation in uterine leiomyoma. Reprod Biol Endocrinol 16, 46. [PubMed: 29747655]

Caterina JJ, Yamada S, Caterina NC, Longenecker G, Holmback K, Shi J, Yermovsky AE, Engler JA, Birkedal-Hansen H, 2000 Inactivating mutation of the mouse tissue inhibitor of metalloproteinases-2(Timp-2) gene alters proMMP-2 activation. J Biol Chem 275, 26416–26422. [PubMed: 10827176]

Driscoll KE, Costa DL, Hatch G, Henderson R, Oberdorster G, Salem H, Schlesinger RB, 2000 Intratracheal instillation as an exposure technique for the evaluation of respiratory tract toxicity: uses and limitations. Toxicol Sci 55, 24–35. [PubMed: 10788556]

Fan X, Wang E, Wang X, Cong X, Chen X, 2014 MicroRNA-21 is a unique signature associated with coronary plaque instability in humans by regulating matrix metalloproteinase-9 via reversion-inducing cysteine-rich protein with Kazal motifs. Exp Mol Pathol 96, 242–249. [PubMed: 24594117]

Feng L, Zhang Y, Jiang M, Mo Y, Wan R, Jia Z, Tollerud DJ, Zhang X, Zhang Q, 2015 Up-regulation of Gadd45alpha after exposure to metal nanoparticles: the role of hypoxia inducible factor 1alpha. Environ Toxicol 30, 490–499. [PubMed: 24277352]

Foldbjerg R, Olesen P, Hougaard M, Dang DA, Hoffmann HJ, Autrup H, 2009 PVP-coated silver nanoparticles and silver ions induce reactive oxygen species, apoptosis and necrosis in THP-1 monocytes. Toxicol Lett 190, 156–162. [PubMed: 19607894]

Gabriely G, Wurdinger T, Kesari S, Esau CC, Burchard J, Linsley PS, Krichevsky AM, 2008 MicroRNA 21 promotes glioma invasion by targeting matrix metalloproteinase regulators. Mol Cell Biol 28, 5369–5380. [PubMed: 18591254]

Galdiero S, Falanga A, Vitiello M, Cantisani M, Marra V, Galdiero M, 2011 Silver nanoparticles as potential antiviral agents. Molecules 16, 8894–8918. [PubMed: 22024958]

Geissmann F, Jung S, Littman DR, 2003 Blood monocytes consist of two principal subsets with distinct migratory properties. Immunity 19, 71–82. [PubMed: 12871640]

Giovannetti E, Funel N, Peters GJ, Del Chiaro M, Erozenci LA, Vasile E, Leon LG, Pollina LE, Groen A, Falcone A, Danesi R, Campani D, Verheul HM, Boggi U, 2010 MicroRNA-21 in pancreatic cancer: correlation with clinical outcome and pharmacologic aspects underlying its role in the modulation of gemcitabine activity. Cancer Res 70, 4528–4538. [PubMed: 20460539]

Greenlee KJ, Werb Z, Kheradmand F, 2007 Matrix metalloproteinases in lung: multiple, multifarious, and multifaceted. Physiol Rev 87, 69–98. [PubMed: 17237343]

He J, Jiang BH, 2016 Interplay between Reactive oxygen Species and MicroRNAs in Cancer. Curr Pharmacol Rep 2, 82–90. [PubMed: 27284501]

Hoesel B, Schmid JA, 2013 The complexity of NF-kappaB signaling in inflammation and cancer. Mol Cancer 12, 86. [PubMed: 23915189]

Imran Din M, Rani A, 2016 Recent Advances in the Synthesis and Stabilization of Nickel and Nickel Oxide Nanoparticles: A Green Adeptness. Int J Anal Chem 2016, 3512145. [PubMed: 27413375]

Itoh Y, Takamura A, Ito N, Maru Y, Sato H, Suenaga N, Aoki T, Seiki M, 2001 Homophilic complex formation of MT1-MMP facilitates proMMP-2 activation on the cell surface and promotes tumor cell invasion. EMBO J 20, 4782–4793. [PubMed: 11532942]

Johnston HJ, Hutchison G, Christensen FM, Peters S, Hankin S, Stone V, 2010 A review of the in vivo and in vitro toxicity of silver and gold particulates: particle attributes and biological mechanisms responsible for the observed toxicity. Crit Rev Toxicol 40, 328–346. [PubMed: 20128631]

Journeay WS, Goldman RH, 2014 Occupational handling of nickel nanoparticles: a case report. Am J Ind Med 57, 1073–1076. [PubMed: 24809594]

Kale SN, Jadhav AD, Verma S, Koppikar SJ, Kaul-Ghanekar R, Dhole SD, Ogale SB, 2012 Characterization of biocompatible NiCo2O4 nanoparticles for applications in hyperthermia and drug delivery. Nanomedicine 8, 452–459. [PubMed: 21839056]

Krek A, Grun D, Poy MN, Wolf R, Rosenberg L, Epstein EJ, MacMenamin P, da Piedade I, Gunsalus KC, Stoffel M, Rajewsky N, 2005 Combinatorial microRNA target predictions. Nat Genet 37, 495–500. [PubMed: 15806104]

Krichevsky AM, Gabriely G, 2009 miR-21: a small multi-faceted RNA. J Cell Mol Med 13, 39–53. [PubMed: 19175699]

Lei D, Lee DC, Magasinski A, Zhao E, Steingart D, Yushin G, 2016 Performance Enhancement and Side Reactions in Rechargeable Nickel-Iron Batteries with Nanostructured Electrodes. ACS Appl Mater Interfaces 8, 2088–2096. [PubMed: 26720271]

Lewis BP, Burge CB, Bartel DP, 2005 Conserved seed pairing, often flanked by adenosines, indicates that thousands of human genes are microRNA targets. Cell 120, 15–20. [PubMed: 15652477]

Li L, Li H, 2013 Role of microRNA-mediated MMP regulation in the treatment and diagnosis of malignant tumors. Cancer Biol Ther 14, 796–805. [PubMed: 23917402]

Ling M, Li Y, Xu Y, Pang Y, Shen L, Jiang R, Zhao Y, Yang X, Zhang J, Zhou J, Wang X, Liu Q, 2012 Regulation of miRNA-21 by reactive oxygen species-activated ERK/NF-kappaB in arsenite-induced cell transformation. Free Radic Biol Med 52, 1508–1518. [PubMed: 22387281]

Livak KJ, Schmittgen TD, 2001 Analysis of relative gene expression data using real-time quantitative PCR and the 2(-Delta Delta C(T)) Method. Methods 25, 402–408. [PubMed: 11846609]

Loffler D, Brocke-Heidrich K, Pfeifer G, Stocsits C, Hackermuller J, Kretzschmar AK, Burger R, Gramatzki M, Blumert C, Bauer K, Cvijic H, Ullmann AK, Stadler PF, Horn F, 2007 Interleukin-6 dependent survival of multiple myeloma cells involves the Stat3-mediated induction of microRNA-21 through a highly conserved enhancer. Blood 110, 1330–1333. [PubMed: 17496199]

Long G, Mo Y, Zhang Q, Jiang M, 2019 Analysis of Nanomaterial Toxicity by Western Blot. Methods Mol Biol 1894, 161–169. [PubMed: 30547461]

Lu AH, Salabas EL, Schuth F, 2007 Magnetic nanoparticles: synthesis, protection, functionalization, and application. Angew Chem Int Ed Engl 46, 1222–1244. [PubMed: 17278160]

Ma X, Becker Buscaglia LE, Barker JR, Li Y, 2011a MicroRNAs in NF-kappaB signaling. J Mol Cell Biol 3, 159–166. [PubMed: 21502305]

Ma X, Kumar M, Choudhury SN, Becker Buscaglia LE, Barker JR, Kanakamedala K, Liu MF, Li Y, 2011b Loss of the miR-21 allele elevates the expression of its target genes and reduces tumorigenesis. Proc Natl Acad Sci U S A 108, 10144–10149. [PubMed: 21646541]

Maxwell P, Salnikow K, 2004 HIF-1: an oxygen and metal responsive transcription factor. Cancer Biol Ther 3, 29–35. [PubMed: 14726713]

Mo Y, Jiang M, Zhang Y, Wan R, Li J, Zhong CJ, Li H, Tang S, Zhang Q, 2019a Comparative mouse lung injury by nickel nanoparticles with differential surface modification. J Nanobiotechnology 17, 2. [PubMed: 30616599]

Mo Y, Wan R, Chien S, Tollerud DJ, Zhang Q, 2009a Activation of endothelial cells after exposure to ambient ultrafine particles: the role of NADPH oxidase. Toxicol Appl Pharmacol 236, 183–193. [PubMed: 19371610]

Mo Y, Wan R, Feng L, Chien S, Tollerud DJ, Zhang Q, 2012 Combination effects of cigarette smoke extract and ambient ultrafine particles on endothelial cells. Toxicol In Vitro 26, 295–303. [PubMed: 22178768]

Mo Y, Wan R, Wang J, Chien S, Tollerud DJ, Zhang Q, 2009b Diabetes is associated with increased sensitivity of alveolar macrophages to urban particulate matter exposure. Toxicology 262, 130–137. [PubMed: 19505525]

Mo Y, Zhang Y, Wan R, Jiang M, Xu Y, Zhang Q, 2020 miR-21 mediates nickel nanoparticle-induced pulmonary injury and fibrosis. Nanotoxicology, In press.

Mo Y, Zhang Y, Zhang Q, 2019b Evaluation of Pulmonary Toxicity of Nanoparticles by Bronchoalveolar Lavage. Methods Mol Biol 1894, 313–322. [PubMed: 30547469]

Mo Y, Zhu X, Hu X, Tollerud DJ, Zhang Q, 2008 Cytokine and NO release from peripheral blood neutrophils after exposure to metal nanoparticles: in vitro and ex vivo studies. Nanotoxicology 2, 79–87.

Moriyama T, Ohuchida K, Mizumoto K, Yu J, Sato N, Nabae T, Takahata S, Toma H, Nagai E, Tanaka M, 2009 MicroRNA-21 modulates biological functions of pancreatic cancer cells including their proliferation, invasion, and chemoresistance. Mol Cancer Ther 8, 1067–1074. [PubMed: 19435867]

Morrissey MA, Sherwood DR, 2015 An active role for basement membrane assembly and modification in tissue sculpting. J Cell Sci 128, 1661–1668. [PubMed: 25717004]

Murphy A, Casey A, Byrne G, Chambers G, Howe O, 2016 Silver nanoparticles induce pro-inflammatory gene expression and inflammasome activation in human monocytes. J Appl Toxicol 36, 1311–1320. [PubMed: 26968431]

Nagase H, Visse R, Murphy G, 2006 Structure and function of matrix metalloproteinases and TIMPs. Cardiovasc Res 69, 562–573. [PubMed: 16405877]

Nemmar A, Hoet PH, Vanquickenborne B, Dinsdale D, Thomeer M, Hoylaerts MF, Vanbilloen H, Mortelmans L, Nemery B, 2002 Passage of inhaled particles into the blood circulation in humans. Circulation 105, 411–414. [PubMed: 11815420]

Nemmar A, Hoylaerts MF, Hoet PH, Vermylen J, Nemery B, 2003 Size effect of intratracheally instilled particles on pulmonary inflammation and vascular thrombosis. Toxicol Appl Pharmacol 186, 38–45. [PubMed: 12583991]

Nemmar A, Vanbilloen H, Hoylaerts MF, Hoet PH, Verbruggen A, Nemery B, 2001 Passage of intratracheally instilled ultrafine particles from the lung into the systemic circulation in hamster. Am J Respir Crit Care Med 164, 1665–1668. [PubMed: 11719307]

Niu J, Shi Y, Tan G, Yang CH, Fan M, Pfeffer LM, Wu ZH, 2012 DNA damage induces NF-kappaB-dependent microRNA-21 up-regulation and promotes breast cancer cell invasion. J Biol Chem 287, 21783–21795. [PubMed: 22547075]

Nothnick WB, Soloway P, Curry TE Jr., 1997 Assessment of the role of tissue inhibitor of metalloproteinase-1 (TIMP-1) during the periovulatory period in female mice lacking a functional TIMP-1 gene. Biol Reprod 56, 1181–1188. [PubMed: 9160717]

Nourse J, Braun J, Lackner K, Huttelmaier S, Danckwardt S, 2018 Large-scale identification of functional microRNA targeting reveals cooperative regulation of the hemostatic system. J Thromb Haemost 16, 2233–2245. [PubMed: 30207063]

Oberdorster G, Oberdorster E, Oberdorster J, 2005 Nanotoxicology: an emerging discipline evolving from studies of ultrafine particles. Environ Health Perspect 113, 823–839. [PubMed: 16002369]

Oh J, Takahashi R, Kondo S, Mizoguchi A, Adachi E, Sasahara RM, Nishimura S, Imamura Y, Kitayama H, Alexander DB, Ide C, Horan TP, Arakawa T, Yoshida H, Nishikawa S, Itoh Y, Seiki M, Itohara S, Takahashi C, Noda M, 2001 The membrane-anchored MMP inhibitor RECK is a key regulator of extracellular matrix integrity and angiogenesis. Cell 107, 789–800. [PubMed: 11747814]

Overall CM, Wrana JL, Sodek J, 1991 Transcriptional and post-transcriptional regulation of 72-kDa gelatinase/type IV collagenase by transforming growth factor-beta 1 in human fibroblasts. Comparisons with collagenase and tissue inhibitor of matrix metalloproteinase gene expression. J Biol Chem 266, 14064–14071. [PubMed: 1649834]

Parks WC, 2003 Matrix metalloproteinases in lung repair. Eur Respir J Suppl 44, 36s–38s. [PubMed: 14582900]

Parks WC, Shapiro SD, 2001 Matrix metalloproteinases in lung biology. Respir Res 2, 10–19. [PubMed: 11686860]

Phillips JI, Green FY, Davies JC, Murray J, 2010 Pulmonary and systemic toxicity following exposure to nickel nanoparticles. Am J Ind Med 53, 763–767. [PubMed: 20623660]

Rana S, Rawat J, Misra RD, 2005 Anti-microbial active composite nanoparticles with magnetic core and photocatalytic shell: TiO2-NiFe2O4 biomaterial system. Acta Biomater 1, 691–703. [PubMed: 16701850]

Reis ST, Pontes-Junior J, Antunes AA, Dall'Oglio MF, Dip N, Passerotti CC, Rossini GA, Morais DR, Nesrallah AJ, Piantino C, Srougi M, Leite KR, 2012 miR-21 may acts as an oncomir by targeting RECK, a matrix metalloproteinase regulator, in prostate cancer. BMC Urol 12, 14. [PubMed: 22642976]

Ries C, Egea V, Karow M, Kolb H, Jochum M, Neth P, 2007 MMP-2, MT1-MMP, and TIMP-2 are essential for the invasive capacity of human mesenchymal stem cells: differential regulation by inflammatory cytokines. Blood 109, 4055–4063. [PubMed: 17197427]

Ries C, Kolb H, Petrides PE, 1994 Regulation of 92-kD gelatinase release in HL-60 leukemia cells: tumor necrosis factor-alpha as an autocrine stimulus for basal- and phorbol ester-induced secretion. Blood 83, 3638–3646. [PubMed: 8204888]

Ries C, Petrides PE, 1995 Cytokine regulation of matrix metalloproteinase activity and its regulatory dysfunction in disease. Biol Chem Hoppe Seyler 376, 345–355. [PubMed: 7576228]

Rueda-Romero C, Hernandez-Perez G, Ramos-Godinez P, Vazquez-Lopez I, Quintana-Belmares RO, Huerta-Garcia E, Stepien E, Lopez-Marure R, Montiel-Davalos A, Alfaro-Moreno E, 2016 Titanium dioxide nanoparticles induce the expression of early and late receptors for adhesion molecules on monocytes. Part Fibre Toxicol 13, 36. [PubMed: 27338562]

Sager TM, Wolfarth M, Leonard SS, Morris AM, Porter DW, Castranova V, Holian A, 2016 Role of engineered metal oxide nanoparticle agglomeration in reactive oxygen species generation and cathepsin B release in NLRP3 inflammasome activation and pulmonary toxicity. Inhal Toxicol 28, 686–697. [PubMed: 27919184]

Salnikow K, Davidson T, Costa M, 2002 The role of hypoxia-inducible signaling pathway in nickel carcinogenesis. Environ Health Perspect 110 Suppl 5, 831–834. [PubMed: 12426141]

Schrand AM, Rahman MF, Hussain SM, Schlager JJ, Smith DA, Syed AF, 2010 Metal-based nanoparticles and their toxicity assessment. Wiley Interdiscip Rev Nanomed Nanobiotechnol 2, 544–568. [PubMed: 20681021]

Senapati VA, Kumar A, Gupta GS, Pandey AK, Dhawan A, 2015 ZnO nanoparticles induced inflammatory response and genotoxicity in human blood cells: A mechanistic approach. Food Chem Toxicol 85, 61–70. [PubMed: 26146191]

Serbina NV, Jia T, Hohl TM, Pamer EG, 2008 Monocyte-mediated defense against microbial pathogens. Annu Rev Immunol 26, 421–452. [PubMed: 18303997]

Shen G, Li X, Jia YF, Piazza GA, Xi Y, 2013 Hypoxia-regulated microRNAs in human cancer. Acta Pharmacol Sin 34, 336–341. [PubMed: 23377548]

Shin SW, Song IH, Um SH, 2015 Role of Physicochemical Properties in Nanoparticle Toxicity. Nanomaterials (Basel) 5, 1351–1365. [PubMed: 28347068]

Sternlicht MD, Werb Z, 2001 How matrix metalloproteinases regulate cell behavior. Annu Rev Cell Dev Biol 17, 463–516. [PubMed: 11687497]

Swirski FK, Pittet MJ, Kircher MF, Aikawa E, Jaffer FA, Libby P, Weissleder R, 2006 Monocyte accumulation in mouse atherogenesis is progressive and proportional to extent of disease. Proc Natl Acad Sci U S A 103, 10340–10345. [PubMed: 16801531]

Takahashi C, Sheng Z, Horan TP, Kitayama H, Maki M, Hitomi K, Kitaura Y, Takai S, Sasahara RM, Horimoto A, Ikawa Y, Ratzkin BJ, Arakawa T, Noda M, 1998 Regulation of matrix metalloproteinase-9 and inhibition of tumor invasion by the membrane-anchored glycoprotein RECK. Proc Natl Acad Sci U S A 95, 13221–13226. [PubMed: 9789069]

Thulasingam S, Massilamany C, Gangaplara A, Dai H, Yarbaeva S, Subramaniam S, Riethoven JJ, Eudy J, Lou M, Reddy J, 2011 miR-27b*, an oxidative stress-responsive microRNA modulates nuclear factor-kB pathway in RAW 264.7 cells. Mol Cell Biochem 352, 181–188. [PubMed: 21350856]

Wan R, Mo Y, Chien S, Li Y, Li Y, Tollerud DJ, Zhang Q, 2011 The role of hypoxia inducible factor-1alpha in the increased MMP-2 and MMP-9 production by human monocytes exposed to nickel nanoparticles. Nanotoxicology 5, 568–582. [PubMed: 21401309]

Wan R, Mo Y, Zhang X, Chien S, Tollerud DJ, Zhang Q, 2008 Matrix metalloproteinase-2 and −9 are induced differently by metal nanoparticles in human monocytes: The role of oxidative stress and protein tyrosine kinase activation. Toxicol Appl Pharmacol 233, 276–285. [PubMed: 18835569]

Wan R, Mo Y, Zhang Z, Jiang M, Tang S, Zhang Q, 2017 Cobalt nanoparticles induce lung injury, DNA damage and mutations in mice. Part Fibre Toxicol 14, 38. [PubMed: 28923112]

Wang SF, Xie F, Hu RF, 2007 Electrochemical study of brucine on an electrode modified with magnetic carbon-coated nickel nanoparticles. Anal Bioanal Chem 387, 933–939. [PubMed: 17180337]

Wang Z, Juttermann R, Soloway PD, 2000 TIMP-2 is required for efficient activation of proMMP-2 in vivo. J Biol Chem 275, 26411–26415. [PubMed: 10827175]

Yu M, Mo Y, Wan R, Chien S, Zhang X, Zhang Q, 2010 Regulation of plasminogen activator inhibitor-1 expression in endothelial cells with exposure to metal nanoparticles. Toxicol Lett 195, 82–89. [PubMed: 20171267]

Zhang Q, Kusaka Y, Sato K, Mo Y, Fukuda M, Donaldson K, 1998a Toxicity of ultrafine nickel particles in lungs after intratracheal instillation. J Occup Health 40, 171–176.

Zhang Q, Kusaka Y, Sato K, Nakakuki K, Kohyama N, Donaldson K, 1998b Differences in the extent of inflammation caused by intratracheal exposure to three ultrafine metals: role of free radicals. J Toxicol Environ Health A 53, 423–438. [PubMed: 9537280]

Zhang Q, Kusaka Y, Zhu X, Sato K, Mo Y, Kluz T, Donaldson K, 2003 Comparative toxicity of standard nickel and ultrafine nickel in lung after intratracheal instillation. J Occup Health 45, 23–30. [PubMed: 14605425]

Zhang Y, Mo Y, Gu A, Wan R, Zhang Q, Tollerud DJ, 2016 Effects of urban particulate matter with high glucose on human monocytes U937. J Appl Toxicol 36, 586–595. [PubMed: 26179980]

Zhang Y, Wan R, Zhang Q, Mo Y, 2019 Application of Gelatin Zymography in Nanotoxicity Research. Methods Mol Biol 1894, 133–143. [PubMed: 30547459]

Highlights

- Primary monocytes were isolated from mouse peripheral blood
- Nano-Ni upregulated miR-21, MMP-2 and MMP-9, and downregulated RECK in WT monocytes
- Nano-Ni did not cause the above effects in monocytes from miR-21 knock-out mice
- Carbon-coating (Nano-Ni-C) ameliorated Nano-Ni-induced MMP-2/9 upregulation
- miR-21/RECK pathway is involved in Nano-Ni-induced MMP-2/9 production

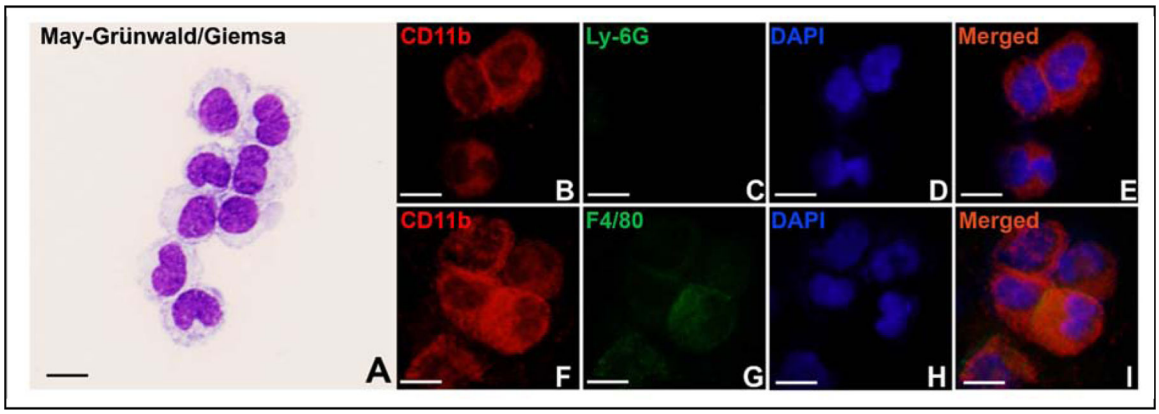

Fig. 1. Isolated monocytes.

Monocytes were isolated from mouse peripheral blood and stained with May-Grünwald and Giemsa stains (**A**), or with anti-CD11b (**B&F**) and anti-Ly-6G (**C**) or anti-F4/80 (**G**) antibodies. DAPI stains the whole nucleus of a cell (**D&H**). **E&I** are merged images. Scale bar represents 10 μm for all panels.

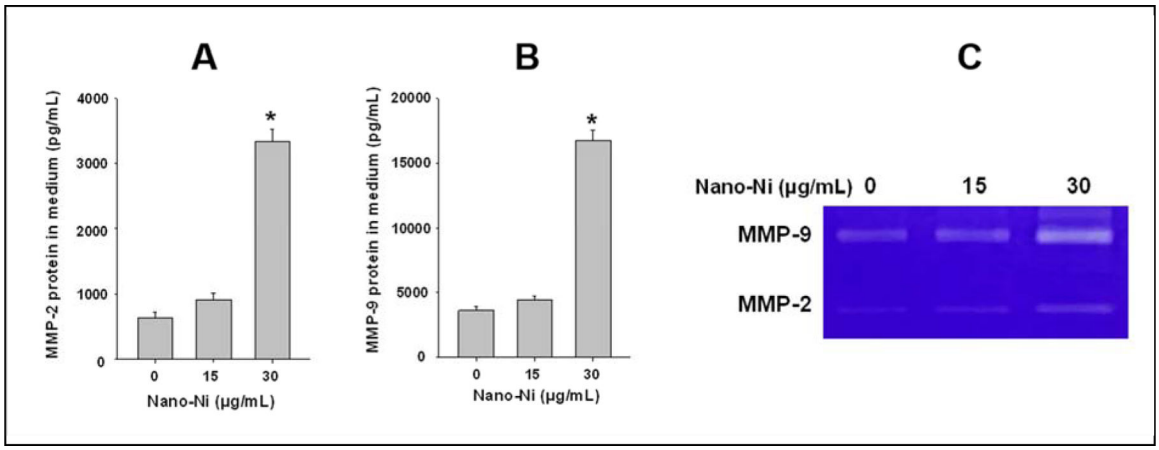

Fig. 2. Dose-response increase of MMP-2 and MMP-9 protein levels and activities in the medium of cultured monocyte after Nano-Ni exposure.

Monocytes were isolated from peripheral blood of wild-type mice and treated with Nano-Ni for 24 h. Cells treated with physiological saline were used as the control. MMP-2 or MMP-9 protein level was determined by Mouse MMP-2 or MMP-9 PicoKine™ ELISA Kit (**A-B**), while MMP-2 and MMP-9 activities were determined by gelatin zymography assay (**C**). Data are shown as mean ± SE (n=3). * $p<0.01$ vs. Control.

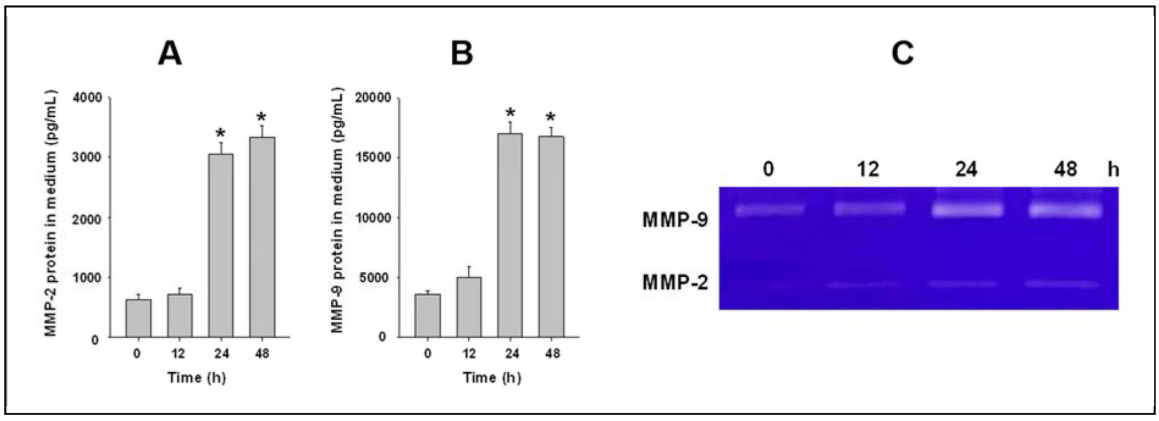

Fig. 3. Time-response increase of MMP-2 and MMP-9 protein levels and activities in the medium of cultured monocyte after Nano-Ni exposure.

Monocytes were isolated from peripheral blood of wild-type mice and treated with 30 μg/mL of Nano-Ni for multiple hours. Cells treated with physiological saline were used as the control. MMP-2 or MMP-9 protein level was determined by Mouse MMP-2 or MMP-9 PicoKine™ ELISA Kit (**A-B**), while MMP-2 and MMP-9 activities were determined by gelatin zymography assay (**C**). Data are shown as mean ± SE (n=3). * $p<0.01$ vs. Control.

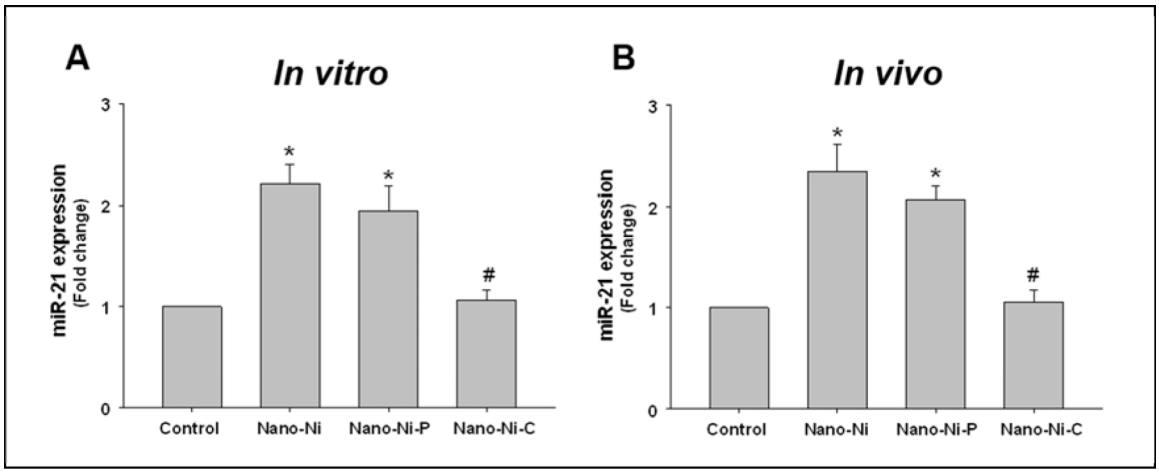

Fig. 4. Upregulation of miR-21 in primary monocytes treated with Nano-Ni and Nano-Ni-P *in vitro* (A) and *in vivo* (B) by real-time PCR.

(**A**) Primary monocytes were isolated from peripheral blood of wild-type mice and treated with 30 μg/mL of Nano-Ni or with either Nano-Ni-P or Nano-Ni-C with same molar concentration of Ni as Nano-Ni for 24 h. Data are shown as mean ± SE (n=3). (**B**) Wild-type mice were intratracheally instilled with 50 μg per mouse of Nano-Ni or with either Nano-Ni-P or Nano-Ni-C with same molar concentration of Ni as Nano-Ni, and monocytes were isolated from peripheral blood at day 3 after exposure. Data are shown as mean ± SE (n=3~6). Cells or mice treated with physiological saline were used as the control. miR-21 expression was determined by real-time PCR and normalized by endogenous control U6 snRNA. * $p<0.05$ vs. Control; # $p<0.05$ vs. Nano-Ni or Nano-Ni-P group.

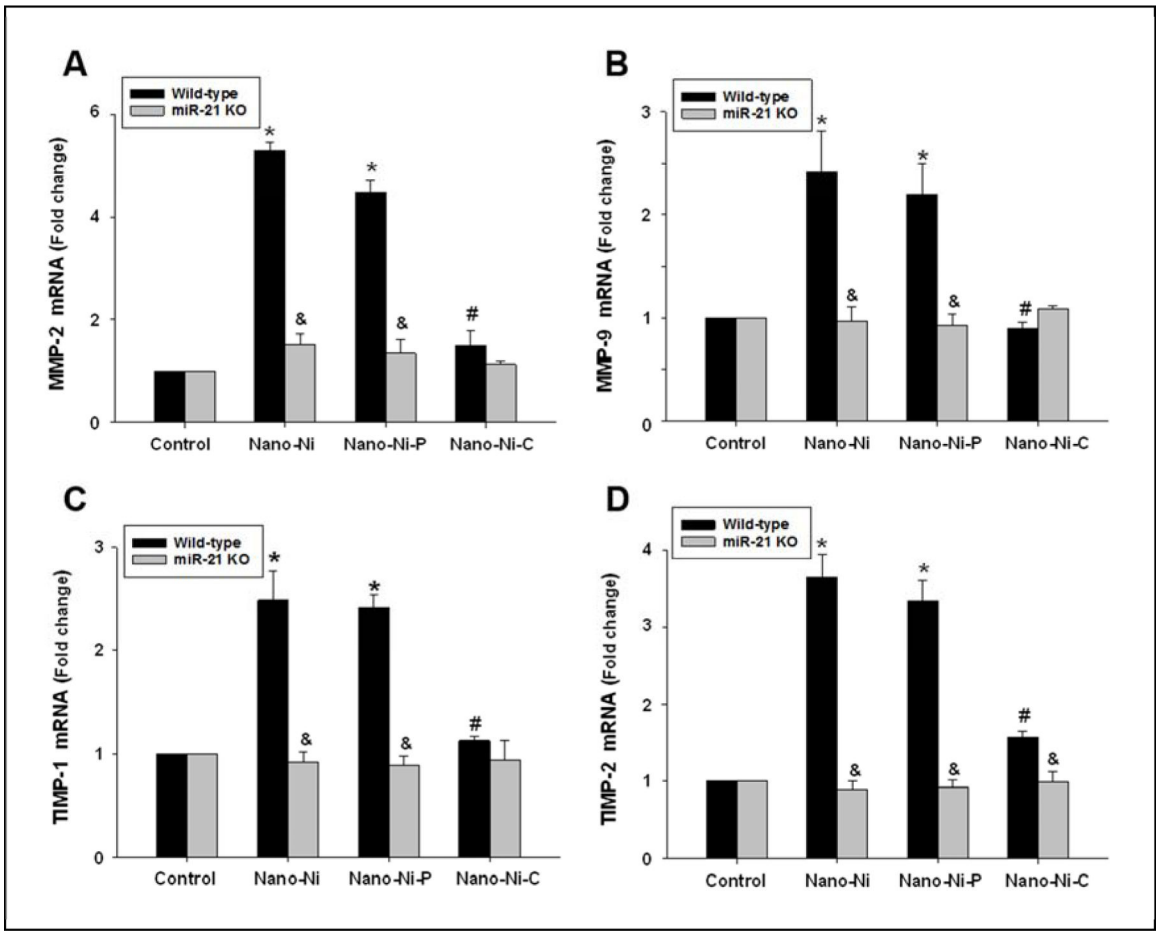

Fig. 5. MMP-2 (A), MMP-9 (B), TIMP-1 (C), and TIMP-2 (D) mRNA expression in mouse monocytes treated with nickel nanoparticles.

Monocytes were isolated from peripheral blood of wild-type or miR-21 KO mice and treated with 30 μg/mL of Nano-Ni or with either Nano-Ni-P or Nano-Ni-C with same molar concentration of Ni as Nano-Ni for 24 h. Cells treated with physiological saline were used as the control. The expression of target gene was determined by real-time PCR and normalized by endogenous control β-actin. Data are shown as mean ± SE (n=3). * $p<0.05$ vs. Control; # $p<0.05$ vs. Nano-Ni or Nano-Ni-P group; & $p<0.05$ vs. wild-type group with the same treatment.

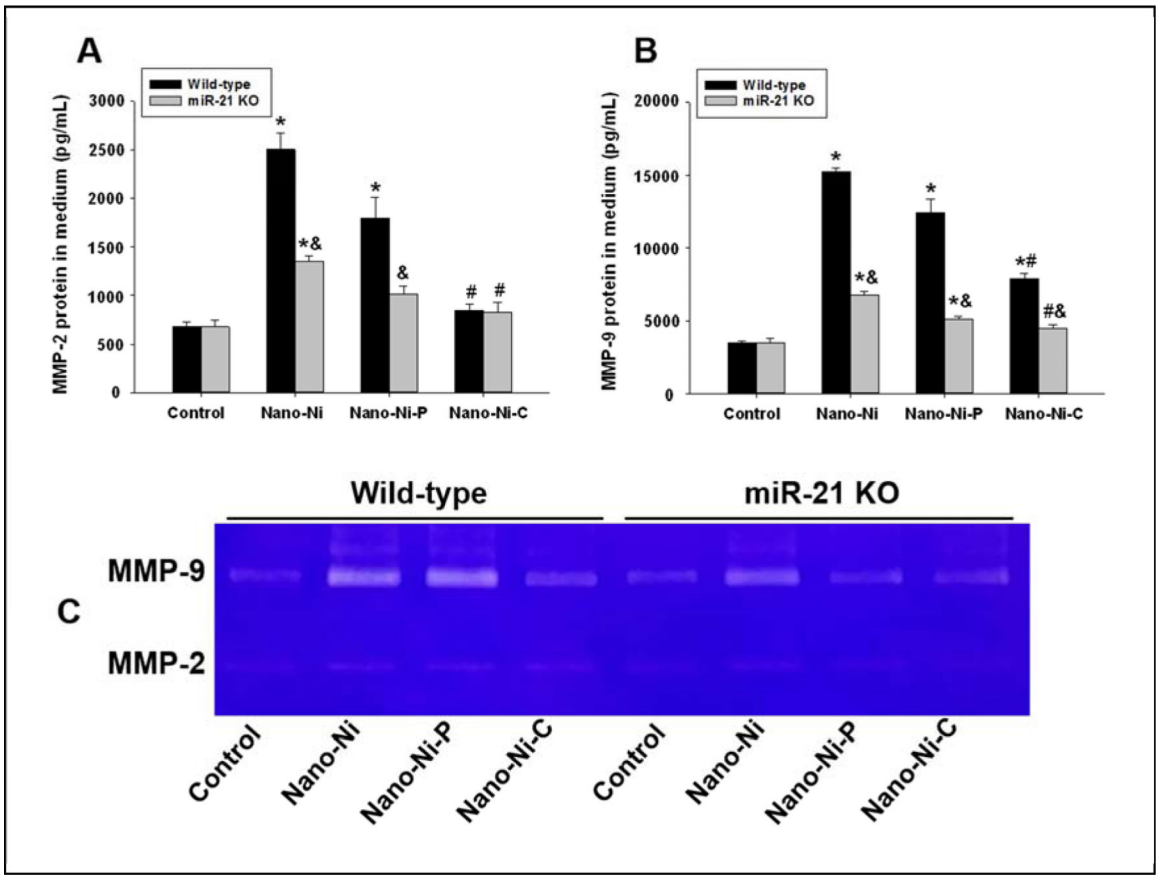

Fig. 6. MMP-2 and MMP-9 protein levels and activities in the monocyte culture medium.

Monocytes were isolated from peripheral blood of wild-type and miR-21 KO mice and treated with 30 μg/mL of Nano-Ni or with either Nano-Ni-P or Nano-Ni-C with same molar concentration of Ni as Nano-Ni for 24 h. Cells treated with physiological saline were used as the control. MMP-2 or MMP-9 protein level was determined by Mouse MMP-2 or MMP-9 PicoKine™ ELISA Kit (**A**-**B**), while MMP-2 and MMP-9 activities were determined by gelatin zymography assay (**C**). Data are shown as mean ± SE (n=3). * $p<0.05$ vs. Control; # $p<0.05$ vs. Nano-Ni group; & $p<0.05$ vs. wild-type group with the same treatment.

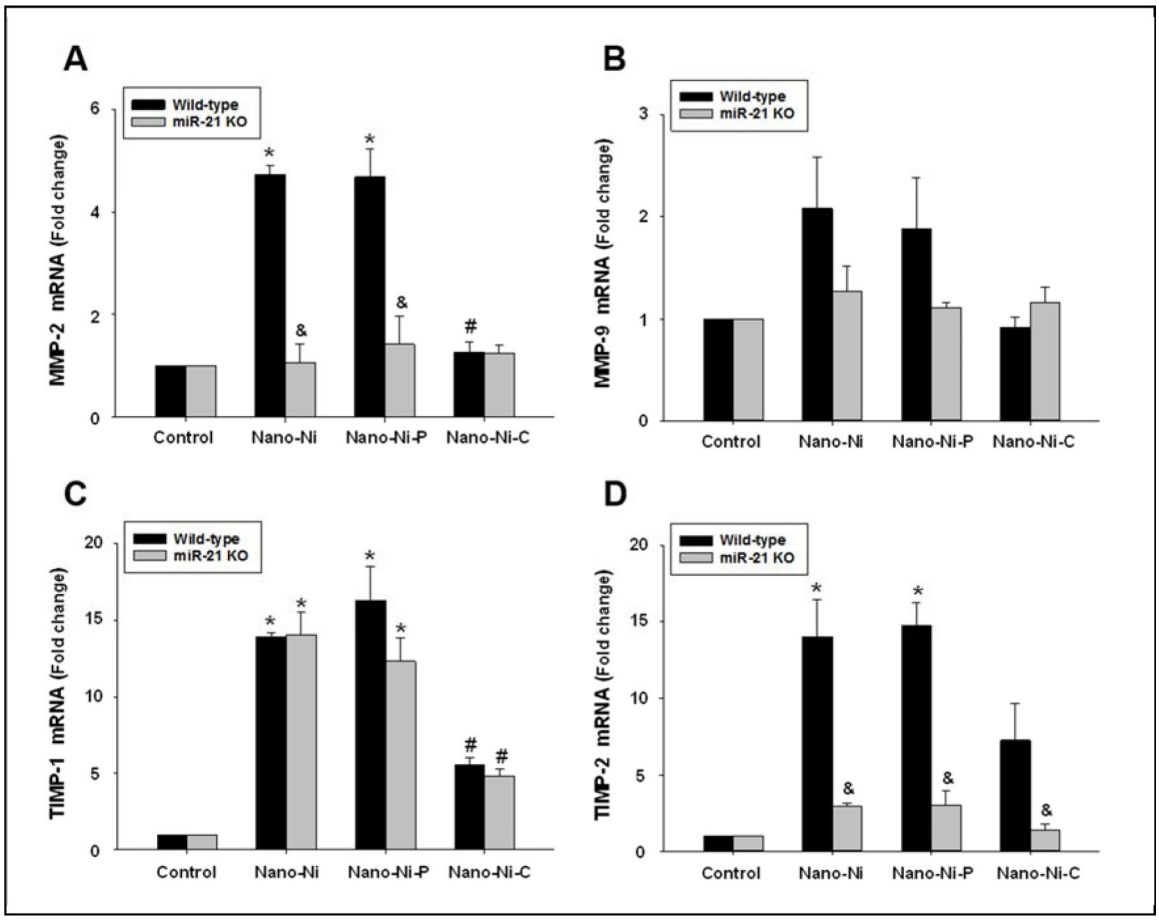

Fig. 7. MMP-2 (A), MMP-9 (B), TIMP-1 (C), and TIMP-2 (D) mRNA expression in monocytes obtained from mice 3 days after nickel nanoparticle treatment.

Wild-type and miR-21 KO mice were intratracheally instilled with 50 μg per mouse of Nano-Ni or with either Nano-Ni-P or Nano-Ni-C with same molar concentration of Ni as Nano-Ni. Control mice were instilled with physiological saline. Monocytes were isolated from mouse peripheral blood at day 3 after exposure. The expression level of the target gene was determined by real-time PCR and normalized by endogenous control GAPDH. Data are shown as mean ± SE (n=3~6). * $p<0.05$ vs. Control; # $p<0.05$ vs. Nano-Ni or Nano-Ni-P group; & $p<0.05$ vs. wild-type group with the same treatment.

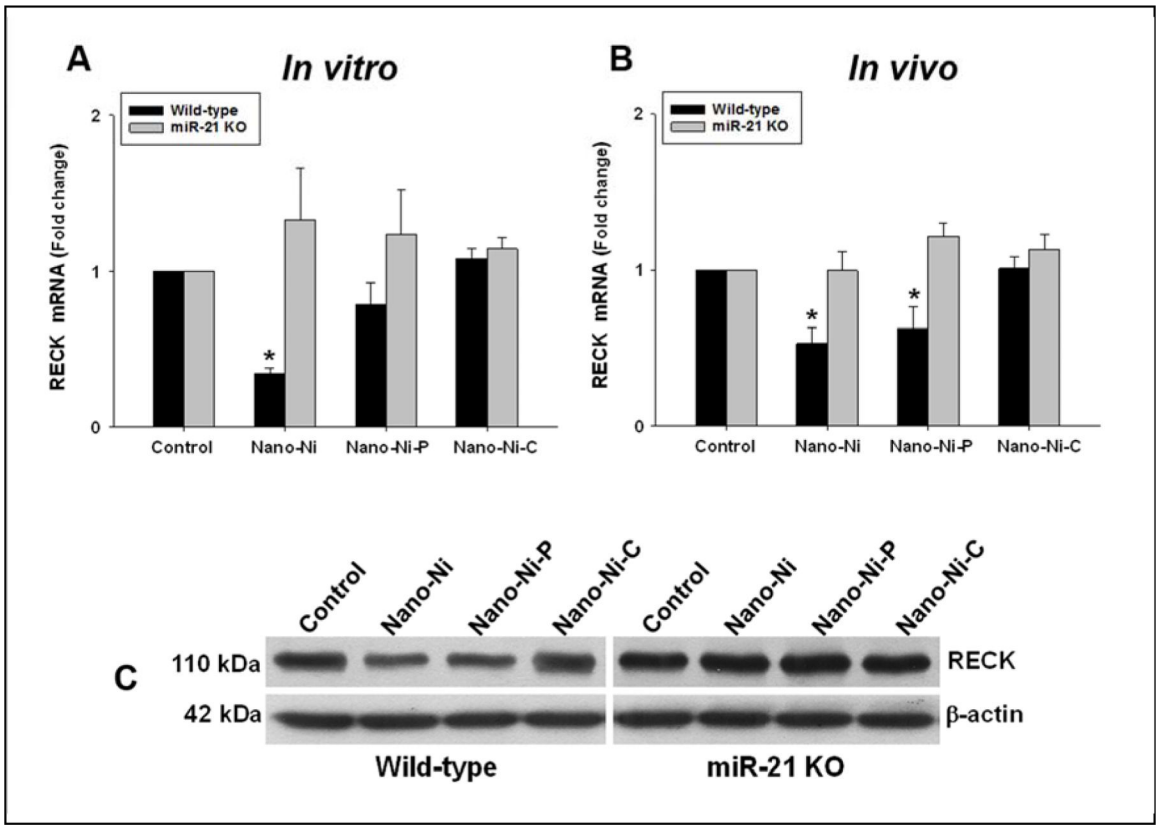

Fig. 8. RECK expression in primary monocytes at *in vitro* (A) and *in vivo* (B) settings.

(**A & C**) Primary monocytes were isolated from peripheral blood of wild-type and miR-21 KO mice and treated with 30 μg/mL of Nano-Ni or with either Nano-Ni-P or Nano-Ni-C with same molar concentration of Ni as Nano-Ni for 24 h. The RECK expression was determined by real-time PCR and normalized by endogenous control bactin (**A**) or by Western blot (**C**). Data are shown as mean ± SE (n=3). * $p<0.05$ vs. Control. (**B**) Wild-type or miR-21 KO mice were intratracheally instilled with 50 μg per mouse of Nano-Ni or with either Nano-Ni-P or Nano-Ni-C with same molar concentration of Ni as Nano-Ni, and monocytes were isolated from peripheral blood at day 3 after exposure. Mice treated with physiological saline were used as the control. The RECK expression was determined by real-time PCR and normalized by endogenous control β-actin. Data are shown as mean ± SE (n=3~6). * $p<0.05$ vs. Control.

Table 1.

Mouse primers used for real-time PCR.

Gene	Forward (5’ → 3’)	Reverse (5’ → 3’)
MMP-2	CCA ACT ACG ATG ATG AC	ACC AGT GTC AGT ATC AG
MMP-9	ACC ACC ACA ACT GAA CCA CA	ACC AAC CGT CCT TGA AGA AA
TIMP-1	ACC ACC TTA TAC CAG CGT TA	AAA CAG GGA AAC ACT GTG CA
TIMP-2	CAC CCG CAA CAG GCG TTT TG	ATC TTG CCA TCT CCT TCT GC
RECK	CTC CAG CAG TCT CCC GTC AT	GTT GTG GGT GGT CAG GGT CTA
GAPDH	TGA AGG TCG GTG TGA ACG GAT TTG GC	CAT GTA GGC CAT GAG GTC CAC CAC
β-actin	GGC ATT GTT ACC AAC TGG GAC	ACC AGA GGC ATA CAG GGA CAG